

## Article

# Effect of Ni Addition on the Interfacial Strength of Al/Cu Dissimilar Welds Produced by Friction Stir Lap Welding

Kota Kurabayashi, Shun Tokita and Yutaka S. Sato \* 

Department of Materials Processing, Graduate School of Engineering, Tohoku University, 6-6-02 Aramaki-aza-Aoba, Aoba-ku, Sendai 980-8579, Japan; kota.kurabayashi.p7@dc.tohoku.ac.jp (K.K.); shun.tokita.c4@tohoku.ac.jp (S.T.)

\* Correspondence: ytkasato@material.tohoku.ac.jp; Tel.: +81-22-795-7352

**Abstract:** Al/Cu dissimilar joining is a key technology for reducing the weight and cost of electrical components. In this study, the dissimilar friction stir lap welding (FSLW) of a Ni-containing Al alloy to pure Cu was performed, and the effects of the addition of Ni on the weld strength and interfacial microstructure were examined. A thin intermetallic compound (IMC) layer was observed at the Al/Cu weld interface produced by FSLW. The addition of 3 at.% Ni effectively improved the weld strength, although the thickness of the IMC layer increased. The IMC layer formed at the Al/Cu interface without Ni comprised  $\text{CuAl}_2$  and  $\text{Cu}_9\text{Al}_4$  from the pure Al side. In contrast, the IMC layer formed with 3 at.% Ni consisted of  $(\text{Ni,Cu})\text{Al}$ ,  $\text{CuAl}$ , and  $\text{Cu}_9\text{Al}_4$  from the Al side. The addition of Ni eliminated the weak  $\text{CuAl}_2/\text{Cu}_9\text{Al}_4$  interface, thereby improving the weld strength. The results of this study suggest that the strength of the Al/Cu weld can be effectively improved by the thinning of the IMC layer caused by FSLW and the change in interfacial microstructure caused by Ni addition.

**Keywords:** dissimilar weld; intermetallic compound; friction stir weld; aluminum alloy; copper



**Citation:** Kurabayashi, K.; Tokita, S.; Sato, Y.S. Effect of Ni Addition on the Interfacial Strength of Al/Cu Dissimilar Welds Produced by Friction Stir Lap Welding. *Metals* **2022**, *12*, 453. <https://doi.org/10.3390/met12030453>

Academic Editor: Paolo Ferro

Received: 9 February 2022

Accepted: 2 March 2022

Published: 7 March 2022

**Publisher's Note:** MDPI stays neutral with regard to jurisdictional claims in published maps and institutional affiliations.



**Copyright:** © 2022 by the authors. Licensee MDPI, Basel, Switzerland. This article is an open access article distributed under the terms and conditions of the Creative Commons Attribution (CC BY) license (<https://creativecommons.org/licenses/by/4.0/>).

## 1. Introduction

Multi-material systems have attracted wide attention owing to their improved properties from combining dissimilar materials. Many studies examined the mechanical properties, interfacial microstructure, and corrosion behavior of multi-material systems, such as Al/Fe structure [1–3]. In particular, the multi-material structures of Al and Cu have been widely researched in the field of welding engineering, thereby reducing the cost and weight of electrical components. However, Al–Cu intermetallic compounds (IMCs), such as  $\text{CuAl}_2$ ,  $\text{CuAl}$ , and  $\text{Cu}_9\text{Al}_4$ , form at the Al/Cu dissimilar interface because of the high affinity between Al and Cu [4–8]. Moreover, a significant degradation of the Al/Cu weld strength due to the formation of brittle IMCs during the welding process has been reported as a common problem in many studies [8–11]. Zhou et al. [12] examined the relationship between the thickness of the IMC layer and the welding current (heat input) during pulsed double-electrode gas metal arc welding (DE-GMAW)–brazing of Al to Cu and concluded that the thickness of the IMC layer increased with an increase in the welding current over 35 A, which decreased the Al/Cu weld strength. Zare et al. [13] examined the interfacial microstructure and mechanical properties of Al/Cu dissimilar welds produced by resistance spot welding and reported that an increase in the welding current beyond a critical value decreased the Al/Cu weld strength owing to the formation of a large amount of the  $\text{CuAl}_2$  phase at the weld interface. Therefore, there have been many attempts to improve the weld strength by controlling the thickness of the IMC layer using a low-heat-input welding process. Tan et al. [14] conducted the butt-welding of 5A02 Al alloy to pure Cu using load-controlled friction stir welding (FSW) equipment and showed that the formation of nanoscale, continuous, and uniform IMC layers greatly enhanced the Al/Cu weld strength. Other solid-state welding processes, such as ultrasonic welding, cold roll welding, and

friction stir spot welding (FSSW), have also been shown to effectively reduce the thickness of the IMC layers, successfully improving the Al/Cu weld strength [4,11,15–19].

Alternatively, some studies have reported that the addition of alloying elements is an effective way to improve the mechanical properties of Al/Cu welds [20–26]. Feng et al. [24] performed Al/Cu brazing with Zn–22Al– $x$ Ce filler metals and showed that the shear strength of the Al/Cu joint produced with Zn–22Al–0.05Ce filler metal was higher than that with Zn–22Al. This study showed that the addition of Ce to the Zn–22Al filler metal refined the interfacial microstructure and decreased the thickness of the IMC layer formed in the Al/Cu brazed joint. Yan et al. [26] examined the effect of alloying elements on the mechanical properties of Al/Cu brazed using Al–Si–La–Sr filler metals. They found that the addition of Si and La to the filler metal strengthened the brazed seam region, which led to fracture of the Al base metal. Furuya et al. [27] examined the effect of alloying elements on the weld strength and interfacial microstructure of Al/Cu dissimilar joints produced by laser lap brazing and reported that the addition of Ni to the Al alloy distinctly improved the weld strength through the formation of a (Ni,Cu)Al layer at the weak  $\text{CuAl}_2/\text{Cu}_9\text{Al}_4$  interface. Furuya et al. [28] also examined the effect of alloying elements on the strength of welds produced by gas tungsten arc welding (GTAW) with Al–X filler materials ( $X = \text{Mn}, \text{Si}, \text{Cr}, \text{Zn}, \text{Ni}, \text{or Sn}$ ), showing that the addition of Ni effectively improved the Al/Cu weld strength. These results show that Ni is an effective alloying element for improving the strength of Al/Cu dissimilar fusion welds.

Based on previous studies, the Al/Cu joint strength can be improved by both thinning the IMC layer, resulting from the use of low-heat-input solid-state welding processes, and by adding alloying elements to the weld interface. The combination of these two effective measures might lead to further improving the Al/Cu weld strength, but the combined effect of FSW and the addition of alloying elements on the Al/Cu weld strength has yet to be examined. Some studies examined the effect of Ni interlayer on the mechanical properties of the Al/Cu weld produced by FSW [20,29,30]. Hou et al. [29,30] examined the metallurgical and mechanical properties of friction stir butt-welded joints of Al to Cu via a cold-sprayed Ni interlayer and reported that the Ni coating improved the interfacial strength and ductility of the Al/Cu weld. These studies showed that the Ni interlayer played a role of a diffusional barrier between Al and Cu, and prevented the formation of Al–Cu brittle IMC layer. However, the contribution of Ni addition to the mechanical properties and microstructure of IMC layer formed at the interface of the Al/Cu weld produced by FSW has not been clarified. This study aims to examine the effect of Ni addition on the mechanical properties and formation of IMCs at the Al/Cu dissimilar interface during FSLW.

## 2. Materials and Methods

### 2.1. Materials

The materials used in this study were an O-free Cu C1020 plate with dimensions of  $100 \times 60 \times 2.0 \text{ mm}^3$  and a commercially pure Al (A1070) ingot. Their chemical compositions are listed in Tables 1 and 2, respectively. To examine the effect of Ni on the weld strength and interfacial microstructure, an Al–Ni alloy ingot was fabricated by a conventional casting method, in which the Ni content was adjusted to 1, 3, and 5 at.%. The A1070 ingot with pure Ni powder was melted at 1173 K in an electric furnace (Yamato Scientific, Tokyo, Japan). After the molten metal was homogenized by stirring, it was cast into a metal mold. The cast Al–Ni alloy was rolled to a thickness of 2 mm at room temperature and cut into pieces with the same dimensions as those of the C1020 plate. The average Vickers hardness values of Cu and cast Al alloy with 0, 1, 3, and 5 at.% Ni were 47, 22, 33, 47, and 49 HV, respectively.

**Table 1.** Chemical composition of C1020.

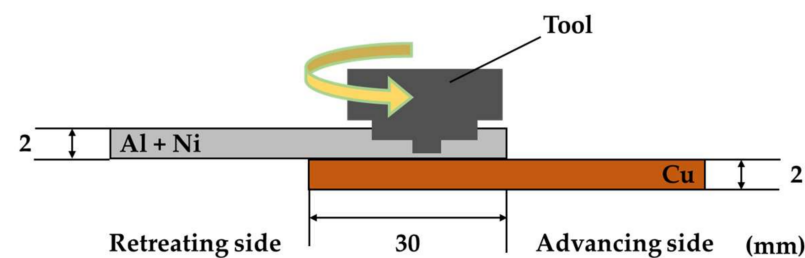
Element	O	Cu
wt.%	0.0001	99.99

**Table 2.** Chemical composition of A1070.

Element	Si	Fe	Cu	Mn	Ti	Al
wt.%	0.06	0.07	0.00	0.00	0.00	99.87

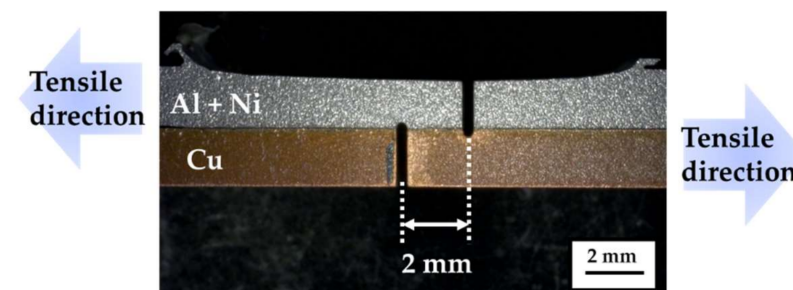
## 2.2. FSW

The Al/Cu plates were lap-welded using a position-controlled FSW machine. A schematic of the Al/Cu dissimilar FSLW process is shown in Figure 1. The Al plate was placed on the Cu plate, and the lap weld was formed by inserting the welding tool into only the Al plate. The welding tool had a shoulder with a diameter of 15 mm and a probe with a diameter and length of 4 and 1.7 mm, respectively. The rotational speed, travel speed, and tilt angle from the plate normal were kept constant at 2000 rpm, 1 mm/s, and 3°, respectively. The plunge depth was controlled to 1.8 mm.

**Figure 1.** Schematic of the Al/Cu dissimilar friction stir lap welding (FSLW) process.

## 2.3. Tensile Shear Test

To examine the Al/Cu weld strength, tensile shear tests were conducted at room temperature with a crosshead speed of 0.3 mm/s using an Instron screw-driven testing machine (Shimadzu, Kyoto, Japan). Tensile specimens with a gauge width of 10 mm were cut perpendicular to the welding direction. To fix the tested area in the tensile specimens to 20 mm<sup>2</sup>, two slits 2 mm apart were made in the Al stir zone and Cu plate using an electrical discharge machine, as shown in Figure 2. Three samples were tested for each Ni content in this experiment, and their strengths were averaged.

**Figure 2.** Locations of the slits in the tensile shear test specimen.

## 2.4. Microstructure Examinations

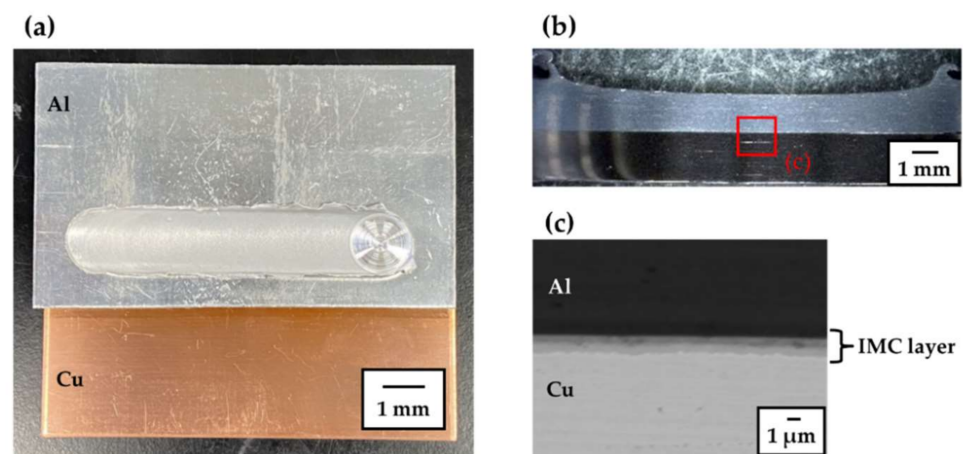
The microstructure of the cross section of the weld was examined by optical microscopy (OM), scanning electron microscopy (SEM, JXA-8530F, JEOL, Akishima, Japan), and transmission electron microscopy (TEM, JEM-2100(HR), JEOL, Akishima, Japan). The thickness of the IMC phases was determined from backscattered electron (BSE) images

obtained by SEM. The IMC phases formed at the interface were identified using TEM with energy-dispersive X-ray spectroscopy (EDS). TEM specimens were prepared using a focused ion beam (FIB, JIB-4600-F, JEOL, Akishima, Japan) system. After the tensile shear tests, the interfaces on the cross sections of the fractured welds were examined by SEM. The phases on the fracture surfaces were examined using X-ray diffraction (XRD) to identify the fracture location of the weld.

### 3. Results and Discussion

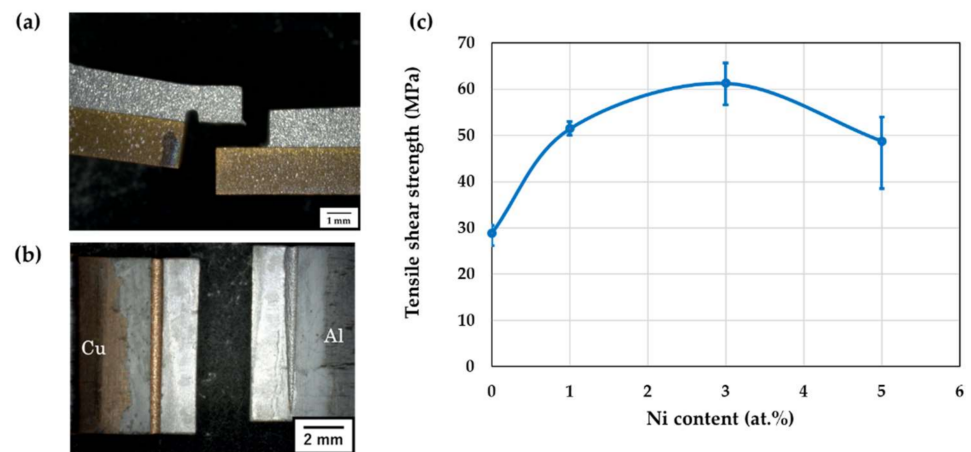
#### 3.1. Weldability and Mechanical Strength of the Joint

Figure 3a shows the typical appearance of the Al/Cu weld produced by FSLW. The surface of the stir zone was smooth without any welding defects, such as voids or flash, and the Ni content of the Al alloy minimally affected the weld quality. A macroscopic overview and the microstructure of the typical Al/Cu dissimilar interface are shown in Figure 3b,c respectively, which show that a defect-free Al/Cu weld was successfully obtained. A continuous IMC layer was observed at the Al/Cu dissimilar interface, which was thicker toward the weld center.



**Figure 3.** (a) Typical appearance of the Al/Cu weld produced by FSLW and (b) macroscopic overview of the cross section and (c) backscattered electron (BSE) image of the Al/Cu dissimilar interface.

The macroscopic overviews of a specimen fractured by tensile shear test are shown in Figure 4a,b. From a macroscopic point of view, all tensile specimens fractured near the interface between the Al stir zone and the Cu plate. Figure 4c shows the relationship between the Ni content of the Al alloy and the tensile shear strength of the Al/Cu weld produced by FSLW. The measurement error was  $\pm 10$  MPa. The tensile shear strength of the joint produced without Ni was approximately 30 MPa, and the addition of Ni effectively improved the Al/Cu weld strength, reaching approximately 60 MPa at 3 at.% Ni. Furuya et al. [28] reported that the addition of 2.3 at.% Ni to the Al/Cu weld produced by GTAW exhibited the most effective improvement in the weld strength, reaching 50 MPa. Therefore, the strength of the Al/Cu weld produced by FSLW was higher than that of the weld produced by GTAW. These results suggest that the addition of an appropriate amount of Ni has the potential to effectively increase the strength of Al/Cu welds produced by FSLW.



**Figure 4.** (a,b) Macroscopic overviews of a fractured specimen and (c) relationship between the tensile shear strength and the Ni content of the Al alloy.

### 3.2. Interfacial Microstructure

Figure 5 shows the BSE images of the Al/Cu dissimilar interface for each Ni content. An interfacial microstructure was observed at the weld center, and the reaction layer formed at the dissimilar interface consisted of several IMCs. Figure 6 shows the relationship between the thickness of the IMC layer and the Ni content of the Al alloy. The thickness of the IMC layer with 3 at.% Ni was 2.4  $\mu\text{m}$ , while without Ni, it was 1.4  $\mu\text{m}$ , indicating that the addition of 3 at.% Ni increased the thickness of the IMC layer. In contrast, it was reported that an IMC layer thicker than 30  $\mu\text{m}$  formed at the interface of an Al/Cu weld produced via GTAW with 2.3 at.% Ni [28]. Because FSW is a low-heat-input joining process, it effectively reduces the thickness of the IMC layer. Many previous studies concluded that a reduction in the IMC layer thickness at the dissimilar interface improves the weld strength [13,31,32]. Thus, the thin IMC layer formed at the Al/Cu interface during FSLW might be a microstructural factor causing the strength of the Al/Cu weld produced by FSLW to be higher than that of the weld obtained by GTAW. However, this study showed that a high weld strength was obtained with a thick IMC layer after FSLW. To clarify this discrepancy, the details of the microstructures of the IMC layers at the Al/Cu weld interface in the Al/Cu welds containing different Ni contents were examined by TEM.

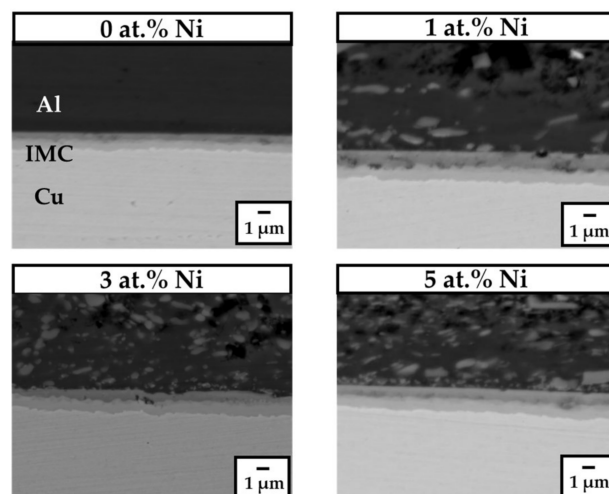


**Figure 5.** BSE images of the Al/Cu dissimilar interface for each Ni content.

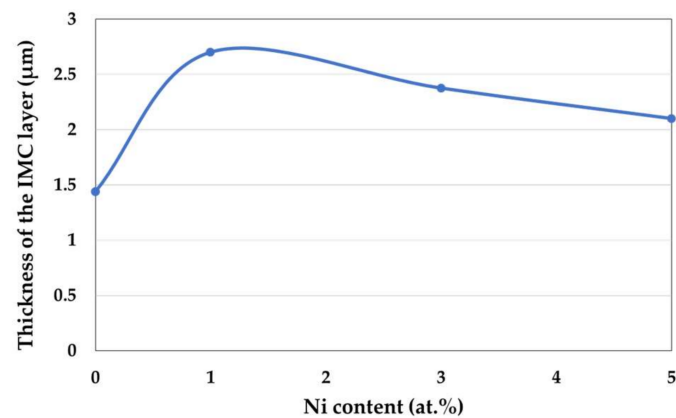


**Figure 6.** Relationship between the thickness of the intermetallic compound (IMC) layer and the Ni content of the Al alloy.

Bright field (BF) TEM and elemental maps of the Al/Cu interface without Ni are shown in Figure 7a, and the selected area electron diffraction (SAED) patterns of the IMC layers formed at the Al/Cu interface are presented in Figure 7b,c. The elemental maps show that the IMC layer consisted of two thin layers. Based on the SAED patterns, these two layers were identified as  $\text{CuAl}_2$  and  $\text{Cu}_9\text{Al}_4$  from the Al side. Some previous studies reported that  $\text{CuAl}_2$  and  $\text{Cu}_9\text{Al}_4$  are the dominant phases formed at the Al/Cu dissimilar interface during FSW [5,9,33]. Guo et al. [34] revealed the preferential formation of  $\text{CuAl}_2$  and  $\text{Cu}_9\text{Al}_4$  at the Al/Cu interface by calculating the driving force for the formation of each IMC. However, improper consolidation, such as voids or cracks, was locally observed at the Al/Cu interface, as shown in Figure 7a, possibly deteriorating the strength of the Al/Cu weld produced by FSW. Improper consolidation may be due to inappropriate welding parameters, but the optimization of the welding parameters was not performed in this study.

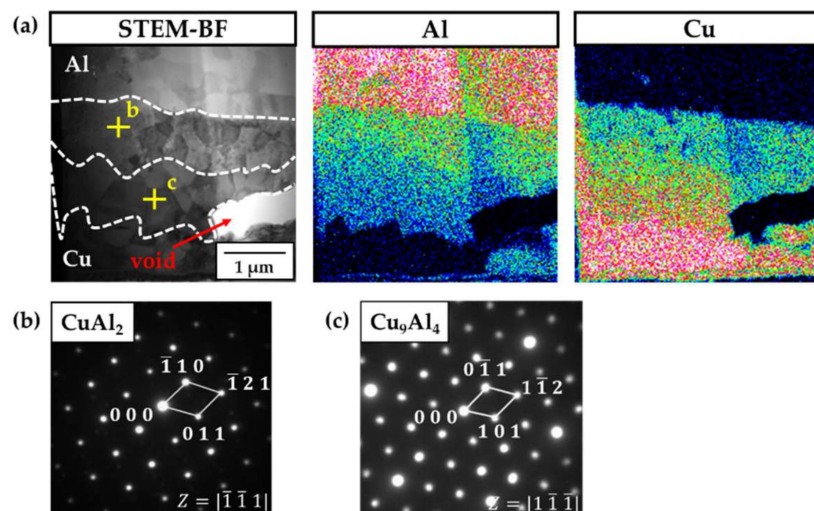


**Figure 7.** (a) Bright field (BF) and elemental maps of the IMC layer formed at the Al/Cu dissimilar interface without Ni and (b,c) corresponding selected area electron diffraction (SAED) patterns.

Figure 8 shows a BF image, elemental maps, and SAED patterns of the IMC layers at the Al/Cu dissimilar interface with 3 at.% Ni. The elemental maps suggest that the IMC layer with the addition of 3 at.% Ni comprised three thin layers. Additionally, the Ni content was high in the IMC layer near the Al side. From the SAED patterns,  $(\text{Ni,Cu})\text{Al}$ ,  $\text{CuAl}$ , and  $\text{Cu}_9\text{Al}_4$  were identified from the Al side. The addition of Ni to the Al/Cu interface changed the IMCs from  $\text{CuAl}_2/\text{Cu}_9\text{Al}_4$  into  $(\text{Ni,Cu})\text{Al}/\text{CuAl}/\text{Cu}_9\text{Al}_4$ . The reason for this change is unclear, but the formation of  $(\text{Ni,Cu})\text{Al}$  may be due to the stabilization of

the B2 phase. (Ni,Cu)Al is a NiAl solid solution with a B2-type structure [35,36]. Based on the Al–Cu–Ni ternary phase diagram, the B2 phase is stable over a wide range of chemical compositions and temperatures. Furuya et al. [27] also reported that (Ni,Cu)Al formed at the Al/Cu interface produced by laser brazing with the addition of Ni, implying that the addition of Ni stabilized (Ni,Cu)Al at the Al/Cu interface. In addition, the change of  $\text{CuAl}_2$  into CuAl due to the addition of Ni may arise from the large amount of Al consumed by the formation of (Ni,Cu)Al.

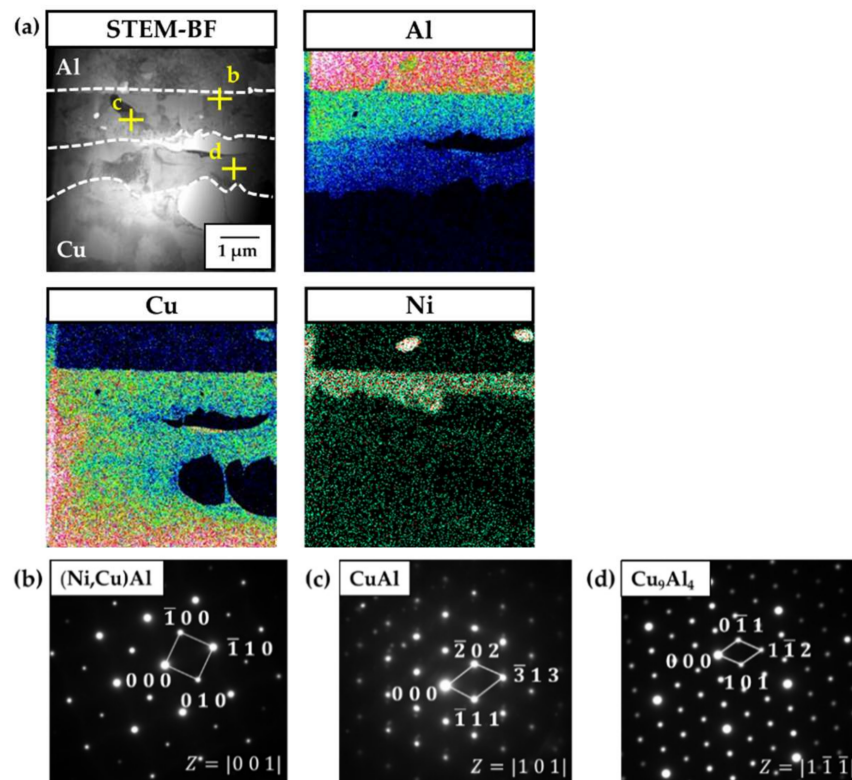


**Figure 8.** (a) BF and elemental maps of the IMC layer formed at the Al/Cu dissimilar interface with 3 at.% Ni and (b–d) corresponding SAED patterns.

### 3.3. Examination of Fracture Location

The BSE images of the interfaces on the cross sections of the fractured tensile specimens produced without Ni and with 3 at.% Ni are shown in Figure 9. The sample without Ni failed at the Al/Cu interface, while a fracture clearly occurred in the Al alloy in the specimen with 3 at.% Ni. To determine the fracture location of the weld without Ni, an XRD analysis was conducted on the fracture surface of the failed specimen. Figure 10 shows the XRD spectra obtained from the fracture surfaces after the tensile shear test. Al peaks overlapped with a small  $\text{CuAl}_2$  peak were detected on the Al side, while a weak  $\text{Cu}_9\text{Al}_4$  peak was found on the Cu side in addition to Cu peaks. Pan et al. [37] reported that an Al/Cu weld failed along the interface between  $\text{CuAl}_2$  and  $\text{Cu}_9\text{Al}_4$  in thin IMC layers. Furuya et al. [27] also reported that the fracture location of the Al/Cu joint produced by laser brazing was the interface between  $\text{CuAl}_2$  and  $\text{Cu}_9\text{Al}_4$ . This implies that the Al/Cu weld without Ni failed at the  $\text{CuAl}_2/\text{Cu}_9\text{Al}_4$  interface.

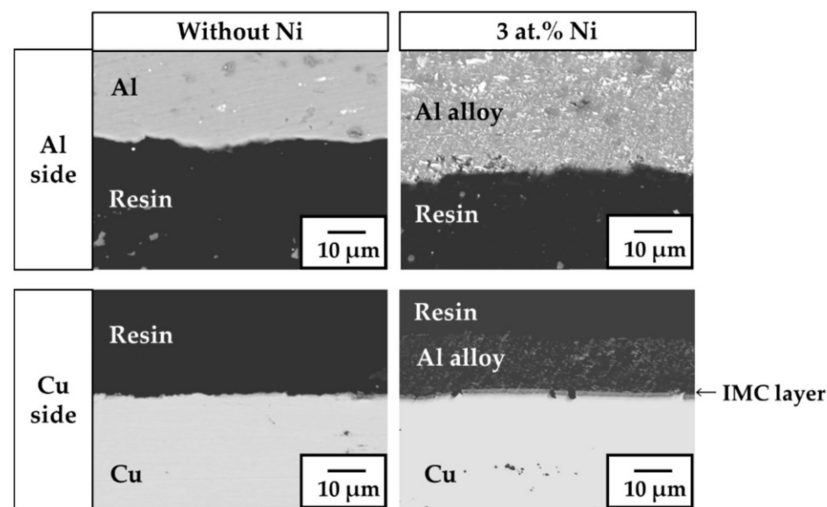


**Figure 9.** BSE images of the interfaces on the cross sections of the fractured Al/Cu welds produced without Ni and with 3 at.% Ni.

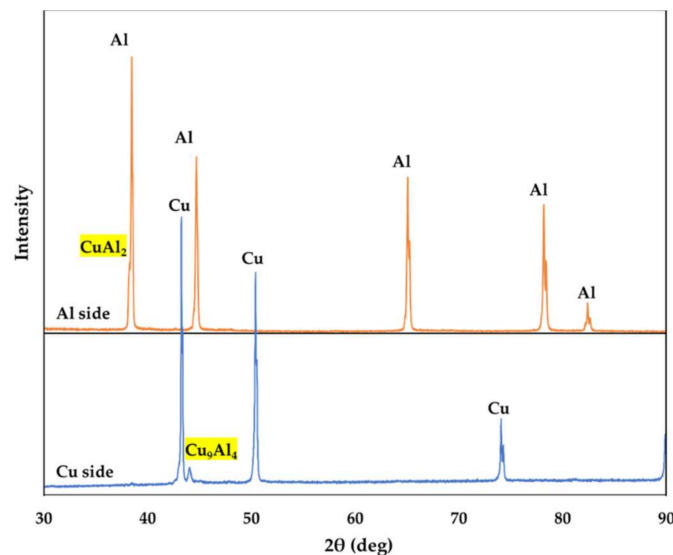


**Figure 10.** X-ray diffraction (XRD) spectra obtained from the fracture surface of the specimen produced without Ni.

### 3.4. Mechanism by Which the Addition of Ni Improved the Weld Strength

The effect of the addition of Ni on the Al/Cu interfacial microstructure and fracture location is illustrated in Figure 11. In the Al/Cu weld without Ni, the IMC layer between pure Al and Cu consisted of  $\text{CuAl}_2$  and  $\text{Cu}_9\text{Al}_4$  from the pure Al side, and the fracture occurred at the interface between  $\text{CuAl}_2$  and  $\text{Cu}_9\text{Al}_4$ . In contrast, the IMC layer formed with the addition of 3 at.% Ni comprised  $(\text{Ni,Cu})\text{Al}$ ,  $\text{CuAl}$ , and  $\text{Cu}_9\text{Al}_4$  from the Al side, and the joint failed in the stir zone of the Al alloy. These results show that the addition of Ni improves the interfacial strength between Al and Cu. Many previous studies on Al/Cu dissimilar welding showed that  $\text{CuAl}_2/\text{Cu}_9\text{Al}_4$  is the weakest interface, which is consistent with the results of this study. The addition of Ni produced  $(\text{Ni,Cu})\text{Al}$  and  $\text{CuAl}$  layers instead of  $\text{CuAl}_2$ , which completely avoided the effect of the weak  $\text{CuAl}_2/\text{Cu}_9\text{Al}_4$  interface on mechanical loading at the Al/Cu interface. Therefore, the addition of Ni improved the strength of the Al/Cu weld produced by FSW.

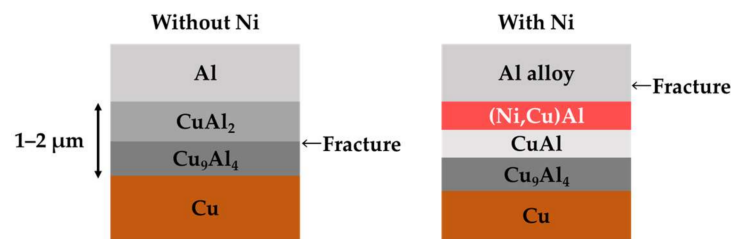


**Figure 11.** Schematic of the Al/Cu dissimilar interface and fracture location of the weld produced by FSW without and with Ni.

Figure 12 shows the effect of Ni addition on the tensile shear strength of Al/Cu dissimilar welds produced by GTAW [28], laser brazing [27], and FSW. Unfortunately, the Al/Cu weld produced by FSLW exhibited a lower strength than that of the welds obtained by GTAW and laser brazing, although it had the thinnest IMC layer. One reason for the low strength of the FSLW joint might be the presence of imperfect consolidation near the Al/Cu interface (Figure 7), which resulted from inappropriate welding parameters. Even after the addition of Ni, the FSLW joint showed a lower strength than that of the laser-brazed joint. The reaction layer formed at the interface during the laser brazing consisted of a  $\text{CuAl}_2 + \text{Al}$  eutectic structure with  $(\text{Ni,Cu})\text{Al}$  particles and  $\text{CuAl}_2$ ,  $(\text{Ni,Cu})\text{Al}$ , and  $\text{Cu}_9\text{Al}_4$  layers from the Al side, and the fracture occurred at the interface between  $\text{CuAl}_2$  and  $(\text{Ni,Cu})\text{Al}$  [27]. In contrast, some dispersoids were observed in the stir zone of the Al alloy in the FSLW joint. It is thought that these dispersoids are  $\text{NiAl}$  and  $\text{NiAl}_3$  that formed during the casting process. They might act as fracture sites in the stir zone of the Al alloy, reducing the strength of the FSLW joint. Therefore, the results of this study suggest that the weld strength can be effectively improved by combining the effect of FSLW and the change in the interfacial microstructure caused by Ni addition.

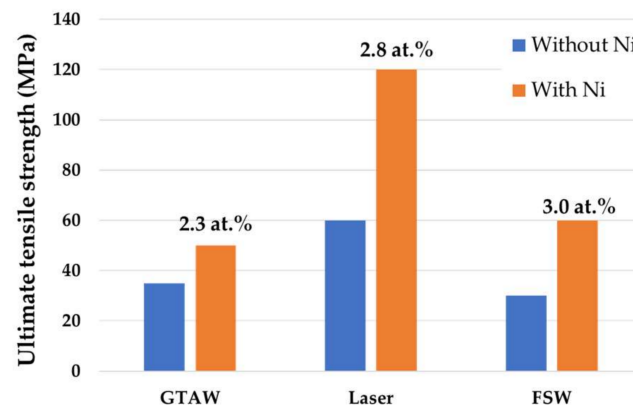


**Figure 12.** Comparison of the ultimate tensile strength of Al/Cu dissimilar welds obtained via gas tungsten arc welding (GTAW), laser brazing and FSW.

#### 4. Conclusions

The effect of the addition of Ni on the strength of the Al/Cu weld produced by FSLW was examined. FSLW effectively reduced the thickness of the IMC layer at the Al/Cu interface. The addition of 3 at.% Ni caused the highest improvement in the weld strength in this study. The addition of 3 at.% Ni changed the IMC phases from  $\text{CuAl}_2/\text{Cu}_9\text{Al}_4$  into  $(\text{Ni,Cu})\text{Al}/\text{CuAl}/\text{Cu}_9\text{Al}_4$  from the Al side. The addition of Ni improved the weld strength through the elimination of the weak  $\text{CuAl}_2/\text{Cu}_9\text{Al}_4$  interface. The results of this study show that the combination of thinning the IMC layer through FSW and changing the interfacial microstructure through Ni addition is an effective method to improve the Al/Cu weld strength.

**Author Contributions:** Conceptualization, Y.S.S.; methodology, K.K. and Y.S.S.; formal analysis, K.K. and S.T.; investigation, K.K.; resources, Y.S.S.; data curation, K.K.; writing—original draft preparation, K.K.; writing—review and editing, Y.S.S. and S.T.; visualization, K.K.; supervision, Y.S.S. and S.T.; project administration, Y.S.S.; funding acquisition, Y.S.S. All authors have read and agreed to the published version of the manuscript.

**Funding:** This research received no external funding.

**Institutional Review Board Statement:** Not applicable.

**Informed Consent Statement:** Not applicable.

**Data Availability Statement:** Not applicable.

**Acknowledgments:** The authors are grateful to K. Kobayashi and K. Sakai for their technical assistance. They also wish to thank S. Omura, K. Sato, K. Yanagisawa, and K.T. Suzuki for their helpful discussions.

**Conflicts of Interest:** The authors declare no conflict of interest.

## References

1. Wang, S.; Zhou, B.; Zhang, X.; Sun, T.; Li, G.; Cui, J. Mechanical properties and interfacial microstructures of magnetic pulse welding joints with aluminum to zinc-coated steel. *Mater. Sci. Eng. A* **2020**, *788*, 139425. [\[CrossRef\]](#)
2. Jiang, H.; Liao, Y.; Jing, L.; Gao, S.; Li, G.; Cui, J. Mechanical properties and corrosion behavior of galvanized steel/Al dissimilar joints. *Arch. Civ. Mech. Eng.* **2021**, *21*, 168. [\[CrossRef\]](#)
3. Liu, Y.; Zhao, H.; Peng, Y. Metallurgical reaction and joining phenomena in friction welded Al/Fe joints. *Int. J. Adv. Manuf. Technol.* **2020**, *107*, 1713–1723. [\[CrossRef\]](#)
4. Abbasi, M.; Karimi Taheri, A.; Salehi, M.T. Growth rate of intermetallic compounds in Al/Cu bimetal produced by cold roll welding process. *J. Alloys Compd.* **2001**, *319*, 233–241. [\[CrossRef\]](#)
5. Genevois, C.; Girard, M.; Huneau, B.; Sauvage, X.; Racineux, G. Interfacial reaction during friction stir welding of Al and Cu. *Metall. Mater. Trans. A* **2011**, *42*, 2290–2295. [\[CrossRef\]](#)
6. Carlone, P.; Astarita, A.; Palazzo, G.S.; Paradiso, V.; Squillace, A. Microstructural aspects in Al-Cu dissimilar joining by FSW. *Int. J. Adv. Manuf. Technol.* **2015**, *79*, 1109–1116. [\[CrossRef\]](#)
7. Abdollah-Zadeh, A.; Saeid, T.; Sazgari, B. Microstructural and mechanical properties of friction stir welded aluminum/copper lap joints. *J. Alloys Compd.* **2008**, *460*, 535–538. [\[CrossRef\]](#)
8. Chen, J.; Lai, Y.S.; Wang, Y.W.; Kao, C.R. Investigation of growth behavior of Al-Cu intermetallic compounds in Cu wire bonding. *Microelectron. Reliab.* **2011**, *51*, 125–129. [\[CrossRef\]](#)
9. Xue, P.; Xiao, B.L.; Ma, Z.Y. Effect of interfacial microstructure evolution on mechanical properties and fracture behavior of friction stir-welded Al-Cu joints. *Metall. Mater. Trans. A* **2015**, *46*, 3091–3103. [\[CrossRef\]](#)
10. Dimatteo, V.; Ascari, A.; Fortunato, A. Continuous laser welding with spatial beam oscillation of dissimilar thin sheet materials (Al-Cu and Cu-Al): Process optimization and characterization. *J. Manuf. Process.* **2019**, *44*, 158–165. [\[CrossRef\]](#)
11. Yang, J.W.; Cao, B.; He, X.C.; Luo, H.S. Microstructure evolution and mechanical properties of Cu-Al joints by ultrasonic welding. *Sci. Technol. Weld. Join.* **2014**, *19*, 500–504. [\[CrossRef\]](#)
12. Zhou, X.; Zhang, G.; Shi, Y.; Zhu, M.; Yang, F. Microstructures and mechanical behavior of aluminum-copper lap joints. *Mater. Sci. Eng. A* **2017**, *705*, 105–113. [\[CrossRef\]](#)
13. Zare, M.; Pouranvari, M. Metallurgical joining of aluminium and copper using resistance spot welding: Microstructure and mechanical properties. *Sci. Technol. Weld. Join.* **2021**, *26*, 461–469. [\[CrossRef\]](#)
14. Tan, C.W.; Jiang, Z.G.; Li, L.Q.; Chen, Y.B.; Chen, X.Y. Microstructural evolution and mechanical properties of dissimilar Al-Cu joints produced by friction stir welding. *Mater. Des.* **2013**, *51*, 466–473. [\[CrossRef\]](#)
15. Heideman, R.; Johnson, C.; Kou, S. Metallurgical analysis of Al/Cu friction stir spot welding. *Sci. Technol. Weld. Join.* **2010**, *15*, 597–604. [\[CrossRef\]](#)
16. Bergmann, J.P.; Petzoldt, F.; Schürer, R.; Schneider, S. Solid-state welding of aluminum to copper—Case studies. *Weld. World* **2013**, *57*, 541–550. [\[CrossRef\]](#)
17. Shiraly, M.; Shamanian, M.; Toroghinejad, M.R.; Jazani, M.A. Effect of tool rotation rate on microstructure and mechanical behavior of friction stir spot-welded Al/Cu composite. *J. Mater. Eng. Perform.* **2014**, *23*, 413–420. [\[CrossRef\]](#)
18. Zhao, Y.Y.; Li, D.; Zhang, Y.S. Effect of welding energy on interface zone of Al-Cu ultrasonic welded joint. *Sci. Technol. Weld. Join.* **2013**, *18*, 354–360. [\[CrossRef\]](#)
19. Wang, K.; Shang, S.L.; Wang, Y.; Vivek, A.; Daehn, G.; Liu, Z.K.; Li, J. Unveiling non-equilibrium metallurgical phases in dissimilar Al-Cu joints processed by vaporizing foil actuator welding. *Mater. Des.* **2020**, *186*, 108306. [\[CrossRef\]](#)
20. Sahu, P.K.; Pal, S.; Pal, S.K. Al/Cu dissimilar friction stir welding with Ni, Ti, and Zn foil as the interlayer for flow control, enhancing mechanical and metallurgical properties. *Metall. Mater. Trans. A* **2017**, *48*, 3300–3317. [\[CrossRef\]](#)

21. Balasundaram, R.; Patel, V.K.; Bhole, S.D.; Chen, D.L. Effect of zinc interlayer on ultrasonic spot welded aluminum-to-copper joints. *Mater. Sci. Eng. A* **2014**, *607*, 277–286. [[CrossRef](#)]
22. Zhou, L.; Luo, L.Y.; Tan, C.W.; Li, Z.Y.; Song, X.G.; Zhao, H.Y.; Huang, Y.X.; Feng, J.C. Effect of welding speed on microstructural evolution and mechanical properties of laser welded-brazed Al/brass dissimilar joints. *Opt. Laser Technol.* **2018**, *98*, 234–246. [[CrossRef](#)]
23. Zhang, M. Effects of interfacial reactions on microstructures and mechanical properties of 3003 Al/T2 Cu and 1035 Al/T2 Cu brazed joints. *Crystals* **2020**, *10*, 248. [[CrossRef](#)]
24. Feng, J.; Songbai, X.; Wei, D. Reliability studies of Cu/Al joints brazed with Zn–Al–Ce filler metals. *Mater. Des.* **2012**, *42*, 156–163. [[CrossRef](#)]
25. Xia, C.; Li, Y.; Puchkov, U.A.; Gerasimov, S.A.; Wang, J. Microstructure and phase constitution near the interface of Cu/Al vacuum brazing using Al–Si filler metal. *Vacuum* **2008**, *82*, 799–804. [[CrossRef](#)]
26. Yan, F.; Xu, D.; Wu, S.C.; Sun, Q.; Wang, C.; Wang, Y. Microstructure and phase constitution near the interface of Cu/3003 torch brazing using Al–Si–La–Sr filler. *J. Mech. Sci. Technol.* **2012**, *26*, 4089–4096. [[CrossRef](#)]
27. Furuya, H.S.; Sato, Y.S.; Kokawa, H.; Huang, T.; Xiao, R.S. Improvement of interfacial strength with the addition of Ni in Al/Cu dissimilar joints produced via laser brazing. *Metall. Mater. Trans. A* **2018**, *49*, 6215–6223. [[CrossRef](#)]
28. Furuya, H.S.; Yabu, S.; Sato, Y.S.; Kokawa, H. Microstructural control of the interface layer for strength enhancement of dissimilar Al/Cu joints via Ni addition during TIG arc brazing. *Metals* **2021**, *11*, 491. [[CrossRef](#)]
29. Hou, W.; Oheil, M.; Shen, Z.; Shen, Y.; Jahed, H.; Gerlich, A. Enhanced strength and ductility in dissimilar friction stir butt welded Al/Cu joints by addition of a cold-spray Ni interlayer. *J. Manuf. Process.* **2020**, *60*, 573–577. [[CrossRef](#)]
30. Hou, W.; Shen, Z.; Huda, N.; Oheil, M.; Shen, Y.; Jahed, H.; Gerlich, A. Enhancing metallurgical and mechanical properties of friction stir butt welded joints of Al–Cu via cold sprayed Ni interlayer. *Mater. Sci. Eng. A* **2021**, *809*, 140992. [[CrossRef](#)]
31. Lee, T.H.; Sim, M.S.; Joo, S.H.; Park, K.T.; Jeong, H.G.; Lee, J.H. Effect of intermetallic compound thickness on anisotropy of Al/Cu honeycomb rods fabricated by hydrostatic extrusion process. *Trans. Nonferrous Met. Soc. China* **2016**, *26*, 456–463. [[CrossRef](#)]
32. Pourabbas, M.; Zadeh, A.A.; Sarvari, M.; Alanagh, F.M.; Pouranvari, M. Role of collision angle during dissimilar Al/Cu magnetic pulse welding. *Sci. Technol. Weld. Join.* **2020**, *25*, 549–555. [[CrossRef](#)]
33. Xue, P.; Xiao, B.L.; Ni, D.R.; Ma, Z.Y. Enhanced mechanical properties of friction stir welded dissimilar Al–Cu joint by intermetallic compounds. *Mater. Sci. Eng. A* **2010**, *527*, 5723–5727. [[CrossRef](#)]
34. Guo, Y.; Liu, G.; Jin, H.; Shi, Z.; Qiao, G. Intermetallic phase formation in diffusion-bonded Cu/Al laminates. *J. Mater. Sci.* **2011**, *46*, 2467–2473. [[CrossRef](#)]
35. Jacobi, H.; Engell, H.J. Defect structure in non-stoichiometric  $\beta$ -(Ni,Cu)Al. *Acta Metall. Mater.* **1971**, *19*, 701–711. [[CrossRef](#)]
36. Kainuma, R.; Liu, X.J.; Ohnuma, I.; Hao, S.M.; Ishida, K. Miscibility gap of B2 phase in NiAl to Cu<sub>3</sub>Al section of the Cu–Al–Ni system. *Intermetallics* **2005**, *13*, 655–661. [[CrossRef](#)]
37. Pan, L.; Li, P.; Hao, X.; Zhou, J.; Dong, H. Inhomogeneity of microstructure and mechanical properties in radial direction of aluminum/copper friction welded joints. *J. Mater. Process. Technol.* **2018**, *255*, 308–318. [[CrossRef](#)]